Separation Controlled Transonic Drag-Rise Modification for V-Shaped Notches

RONALD H. HOWELL*
University of Missouri-Rolla, Rolla, Mo.

AND

HELMUT H. KORST†
University of Illinois at Urbana-Champaign, Urbana, Ill.

Experimental values of drag coefficients of V-shaped notches have been measured and show an anomalous behavior in the transonic regime since they reach maximum values at slightly supersonic Mach numbers with moderate drag increases. This is shown to be caused by the inviscid-viscid interaction controlling flow separation and reattachment. Besides Mach number, the notch geometry and the boundary-layer thickness notch-length ratio were found to be of significance while Reynolds number effects were mild. Results of Schlieren photographs, pressure distribution measurements, and direct drag force measurements for a wide range of flow and geometrical variables are presented.

Nomenclature

b = width of plate or notch
C = Crocco number, velocity/maximum velocity
C_D = drag coefficient, $D\frac{1}{2}\rho_e U^2 bL$
C_f = skin-friction coefficient, $\tau\frac{1}{2}\rho_e U^2$
C_{FN} = experimental notch drag coefficient, $F_N/\frac{1}{2}\rho_e U^2 bL$
d = penetration depth, the vertical distance between top of notch and the separation point
D = drag force
D_{mixing} = drag force due to free shear layer mixing
D_{wave} = drag force due to pressure forces
F = drag force on flat plate of the same length as a notch
F_N = notch drag force
$I_{j\eta_p}$ = $\int_{-\infty}^{\eta_j} \Phi^2 d\eta/(1 - C_e^2\Phi_s)$
J = shear stress function
k = ratio of specific heats
L = notch length
M = Mach number
p = pressure
r = depth of notch
Re_θ = momentum thickness Reynolds number
Re_L = notch length Reynolds number
U = freestream velocity
u = velocity component in x-direction
x = coordinate along plate or notch surface
y = coordinate normal to plate or notch
δ = boundary-layer thickness
η = $y\eta_p/\delta_s$
η_p = position parameter
Ω = notch angle
Φ = velocity ratio, $u/U = \Phi(\Phi_s,\eta,\eta_p)$
ρ = density
τ = shear stress
θ = boundary-layer momentum thickness

Subscripts

e = freestream conditions
j = dividing streamline
s = at separation

Received October 13, 1970; revision received April 12, 1971. This work was supported in part by NASA under Grant NSG 13-59 at the University of Illinois at Urbana-Champaign.

* Associate Professor of Mechanical Engineering.

† Professor and Head, Department of Mechanical and Industrial Engineering.

Index categories: Jets, Wakes, and Viscid-Inviscid Flow Interactions; Subsonic and Transonic Flow; Boundary Layers and Convective Heat Transfer—Turbulent.

I. Introduction

As the speed of a body increases toward sonic velocity and into the supersonic regime the drag coefficient for surface discontinuities such as protuberances, steps, and notches can change by an order of magnitude. For this reason, accurate information about local details in surface configurations is desirable as is the knowledge of the detailed flow mechanisms which determine aerodynamic stress distributions and heat-transfer characteristics near such disturbances.

The subject of the present study is the magnification of the drag force due to the presence of a V-shaped notch in a flat surface. Figure 1a depicts the wall geometry together with the freestream and approaching flow conditions in the boundary layer.

The two-dimensional notches were always symmetrical so that a single angle Ω would completely determine their shape. Freestream conditions could be varied over a range $0.6 < M < 1.14$ in the trasonic regime with additional experiments conducted at $M \simeq 2$. The approaching fully developed boundary layer was always turbulent and the momentum thickness Reynolds number varied from 7,500–15,000. By using notches of different lengths L the ratio of θ/L could be controlled.

Recent literature survey reports[1–3] reveal that no values of direct measured drag force coefficients have been reported in the open literature for symmetrical V-shaped notches exposed to transonic or supersonic flows. However, some pertinent analyses have been conducted which furnish useful direction for dealing with the stated problem. Charwat et al. [4] investigated separated flow regions near rectangular cutouts for a supersonic external stream with an approaching turbulent boundary layer and found that there was a critical value for the ratio of the length of the separated free shear layer to the depth of the cavity beyond which the cavity became two separated regions. Kuehn[5] investigated the generation of pressure changes created by combinations of expansion corners and wedges. The results of these investigations were useful only in a qualitative way since the wall geometry exerts the major influence on the locations of the points of separation and reattachment.

In contrast to rather well defined boundary conditions (walls) for attached flows the occurrence of separation often allows major adjustments in the flow geometry as a consequence of small changes in flow conditions. Where flow separation is a prominent feature, understanding has re-

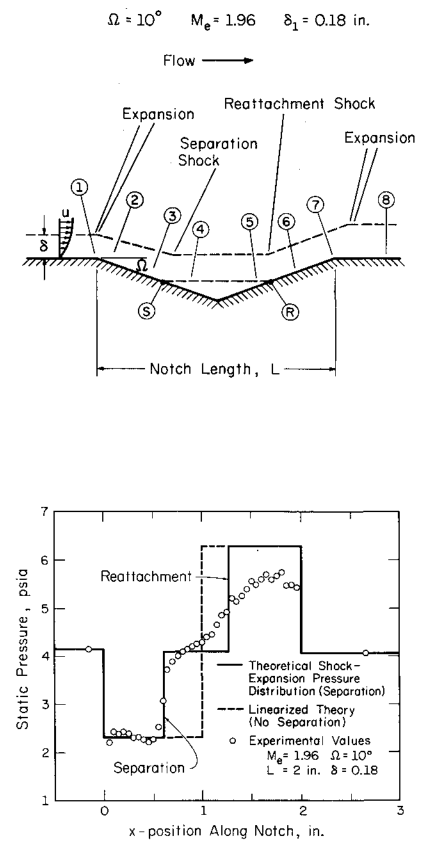

a) **Notch nomenclature.**

b) **Notch pressure distribution.**

Fig. 1 V-notch nomenclature and pressure distribution.

mained incomplete in spite of proposed flow models such as those advanced by Crocco and Lees,[6] Lees and Reeves,[7] Chapman,[8] and Korst.[9]

II. Qualitative Observations Concerning Flow Geometry

Form drag is determined, within certain limitations arising from viscous interactions, by the geometry of the walls. The situation may change considerably, however when there is a region of separated flow such as exists in a V-shaped notch with the wall angle exceeding a limiting value which depends upon approach Mach number and the upstream boundary-layer configurations. For this case, the separation causes the pressure drag to be strongly modified as a consequence of the actual flow geometry (see Fig. 1) being at variance with the wall boundary conditions. This is borne out by Fig. 1b where three different static pressure distributions are shown: 1) the theoretical wall pressure distribution for linearized supersonic flow (in absence of separation) due to Prandtl-Meyer expansions and a shock located at the vertex of the V-notch; 2) the theoretical shock-expansion pressure distribution consistent with the flow model shown, accounting for flow separation; and 3) experimental values obtained for the 10° V-shaped notch.

As noted before, the measured pressure distribution differs greatly from curve 1. As a consequence of separation, the pressure increase at the center of the notch is eased by the interaction between the freestream and shear flow regions. Consequently, it can be recognized that the form drag is not directly related to the wall geometry, but rather to the flow geometry as affected by separation. In comparing 2–3, it is also seen that the viscous layers by themselves are of major interest and introduce an important modifying element to the theoretical shock-expansion model. The qualitative effect of the boundary layer when it is of significant thickness in comparison to the length of the notch is to reduce the drag force. For boundary layers that are thick relative to the notch dimension, the notch is buried under the shear layer. The limiting case for this situation would be when the notch appears only as a surface imperfection for very thick boundary layers ($\delta/L \rightarrow \infty$).

Schlieren photographs[1] of flow over V-notches with increasing notch angle Ω at constant approaching external free-stream Mach number $M_e = 1.14$ and constant values of θ/L and Re_L are shown in Figs. 2a–d. One observes that as Ω increases, the separation point moves upstream while reattachment moves downstream. For the approaching flow conditions used in this investigation, the separation point S was almost at the leading edge of the notch when the angle was greater than 10°; however, the separation point never did move completely down to the vertex of the notch even when the notch angle was reduced to 7°.

The effect of a systematic change in Mach number throughout the transonic regime with θ/L, Re_L, and Ω constant (Schlieren photographs[1]) disclosed that the separation point was nearest the leading edge of the notch near a Mach number equal to unity, while for larger or smaller Mach number the separation point moved farther downstream.

The effect on the flow configuration when θ/L was changed while maintaining a constant Mach number Re_L and notch angle was not noticeable for the relatively small range of values of θ/L. Schlieren photographs were taken of the flow structure over 4-in.-long notches at a Mach number of two and the flow structures were identical to those for 2-in.-long notches even though θ/L was smaller by a factor of one-half.

III. Analysis

An attempt was made to incorporate the qualitative observations concerning flow geometry into a rather simple, phenomenologically conceived model comprising the wave drag of the inviscid streamline configuration and those shear stresses contributed by the mixing shear layer. This concept is reasonably correct as long as the shear force due to the attached boundary layers between Secs. 2 and 3 and between Secs. 6 and 7 in Fig. 1a remain small as compared to the form drag of the wall portions.

It should be noted that the exact locations of either the separation point or the reattachment point are generally not known nor can they be determined presently with sufficient quantitative accuracy by entirely analytical methods. For this analysis, it was assumed that the separation streamline remains practically parallel to the external flow such that a single geometrical parameter, the penetration depth ratio d/r, fully describes the flow geometry of the model ($d/r = 1$ corresponds to attached flow). This penetration depth ratio was strongly dependent upon the parameters controlling the problem and had to be obtained from experiments.

Several methods were used to locate the point of separation inside the V-notches. Schlieren photographs were taken of the flowfields in supersonic and transonic flow[1] for many of the notches tested. From these photographs, approximate separation locations were measured and recorded. For many of the notch shapes, models were constructed with pressure taps along the bottom of the notch so that static pressure distributions could be measured in the notch. A typical notch pressure distribution is shown in Fig. 1b for a 2-in., 10° notch with $M_e = 1.96$. A third method that was used to locate a point of separation was the oil film technique. In this method, a thin film of heavy oil was placed along the separating surface before the test. During the test, a thin line of oil accumulated at the separation point.

The results from all three methods are shown in Fig. 3 for a 2-in. notch. The invididual results from the different techniques are not differentiated in Fig. 3, but the three methods were in close agreement. In the following, the viscous shear forces in the attached boundary layer close to the separation

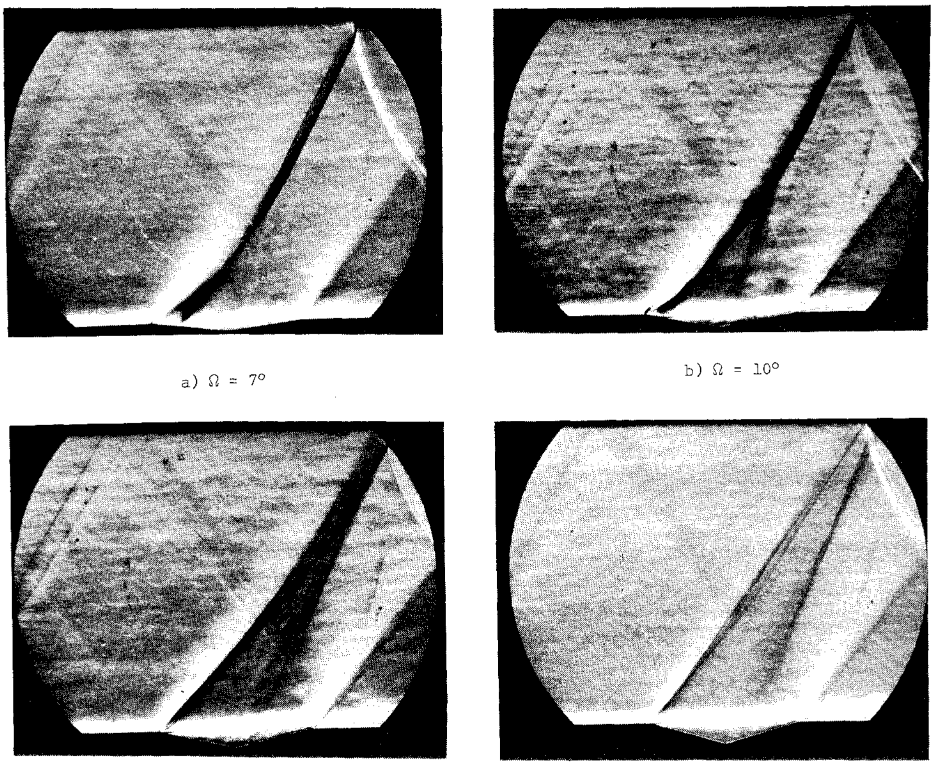

a) Ω = 7° b) Ω = 10°

c) Ω = 13° d) Ω = 16°

Fig. 2 Flow over V-notch (M_e = 1.14, L = 2 in.).

and reattachment regions can be neglected when compared to either the form drag D_{wave} or the viscous drag contribution of the free shear layer D_{mixing}.

A. Supersonic Flow (Linearized)

For the restriction that the Mach number is greater than unity (but not close to unity) and less than ten, linearized supersonic theory can be used to calculate the wave drag on the model. The drag due to pressure forces on the notch is[10]

$$D_{\text{wave}} = \tfrac{1}{2}\rho_e U_e^2 bL(d/L)[4\tan\Omega/(M_e^2 - 1)^{1/2}] \quad (1)$$

The drag force contribution of the separated shear layer (S–R in Fig. 1a) was treated utilizing the method presented by Lamb.[11] The drag force along the dividing streamline is given by

$$D_{\text{mixing}} = b\int_0^x \tau_j\, dx \quad (2)$$

Lamb has shown that Eq. (2) can be rearranged to

$$D_{\text{mixing}} = \rho_e U_e^2(1 - C_e^2)\delta_s b\int_0^\psi J_j\, d\psi \quad (3)$$

The shear stress function J_j is related to the integral $I_{j\eta_p}$ through a position parameter η_p such that

$$D_{\text{mixing}} = \rho_e U_e^2 b(1 - C_e^2)(\delta_s/\eta_p)I_{j\eta_p} \quad (4)$$

Adding D_{wave} and D_{mixing} and substituting the resulting expression into the equation for notch drag coefficient defined

$$C^1 = D/\tfrac{1}{2}\rho_e U^2 bL \quad (5)$$

yields

$$C_D = 2r/L[4/(M_e^2 - 1)^{1/2}(d/L) + (1 - C_e^2)I_{j\eta_p}/\eta_p(\delta_s/r)] \quad (6)$$

B. Low Supersonic Flow Regime

A simplified model for the analysis of the drag force of a V-shaped notch can be constructed for supersonic flow approaching the transonic flow regime (but with $M_e > 1$) if several assumptions are made. First it is assumed that the notch angle is small (less than 10°) so that there is little, if any, separated flow near the vertex of the notch. Then, for d/r equal to unity, a plane shock at the vertex of the notch, and Prandtl-Meyer expansions at the front and rear of the notch, the drag coefficient is given by

$$C_D = [(P_2/P_1) - 1](P_1/P_e)(r/L)/(k/2)M_e^2 \quad (7)$$

The gradual implementation of this flow model to include separation effects can be demonstrated as the change in the flowfield is considered when M_e is decreased from a supersonic value of approximately two toward unity.

According to plane shock theory, when the approach Mach number reaches a lower limiting value (greater than unity and dependent on Ω), the shock wave which has assumed to be located at the vertex of the notch must detach and move up-

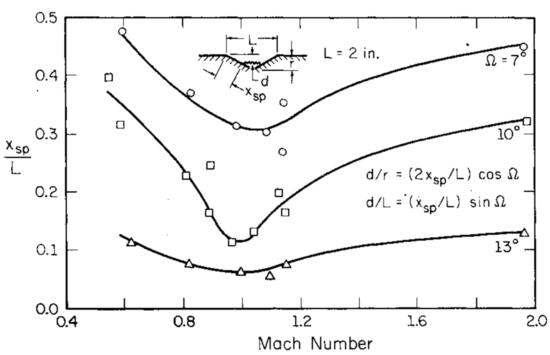

Fig. 3 Self-adjustment of the separation point.

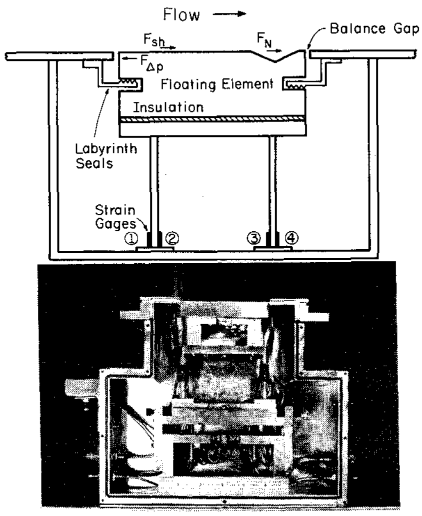

Fig. 4 Drag force balance.

stream. This is exactly the phenomenon which was observed from Schlieren photographs[1] and the location of the separation point, as affected by freestream Mach number and notch angle, as shown in Fig. 3.

Either analysis depends on information concerning d/r which, when extracted from experiments, should produce quantitative drag values. Whether the analytical models are conceptually correct can be borne out only by direct experimental determination of drag coefficients. This has been accomplished by direct drag force measurements in supersonic and transonic wind tunnels which, of course, has been the major objective of the study.

IV. Experimental Investigation

A. Test Facilities

The experimental work has conducted in the supersonic and transonic blowdown wind tunnel operated jointly by the Department of Mechanical and Industrial Engineering and the Department of Aeronautical and Astronautical Engineering at the University of Illinois at Urbana-Champaign, Urbana, Illinois.

The supersonic test section had an area of 8 in.^{2} and could be operated with stagnation pressures between 13 and 60 psig. The stagnation temperature varied between 50°F and 90°F depending on ambient conditions, stagnation pressure, and run time. The test section Mach number was 1.96, but varied slightly with stagnation pressure. At a stagnation pressure of about 30 psia and a stagnation temperature of 50°F, the tunnel had a Reynolds number per foot of 9×10^6.

The transonic rectangular test section had transparent side walls for flow observation, while the top and bottom walls were slotted. For the purpose of the present investigation,

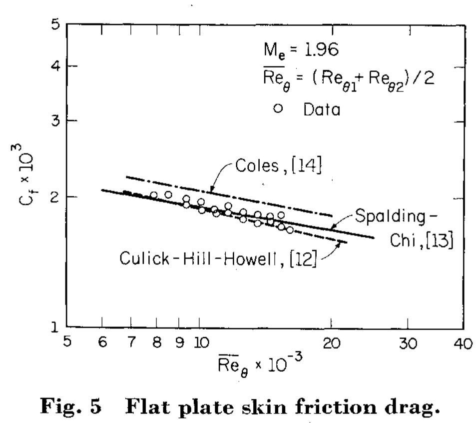

Fig. 5 Flat plate skin friction drag.

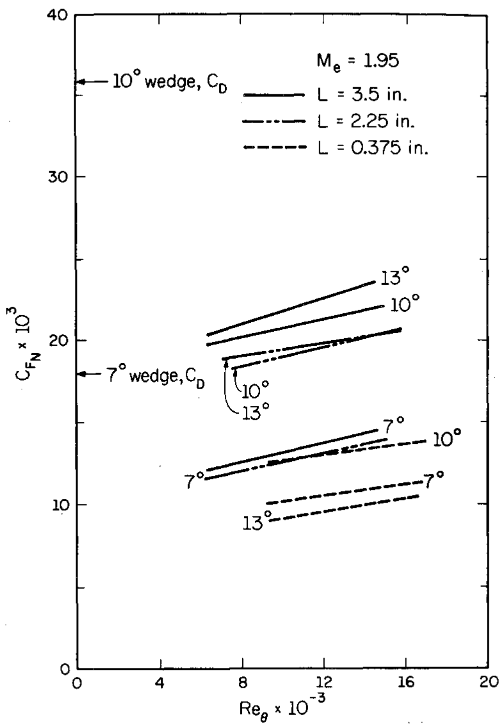

Fig. 6 Summary of supersonic notch drag.

the slotted wall at the bottom was replaced by a solid wall into which the notch models or the balance could be installed. The reduction in the wall permeability was permissible due to the small effective blockage of the models. The Mach number at the test section could be varied from approximately 0.5–1.2 by changing the tunnel stagnation pressure. No direct means of controlling the Reynolds number was possible in this flow regime. The momentum thickness Reynolds number at the beginning of the test section varied from 7800–9500 for the stated Mach number variation. Experiments were conducted using notches of various lengths between 0.375 and 3.5 in. and notch angles of 7, 10, 13, and 16°. All notch models spanned the entire 4 in. width of the test section, but drag forces were only determined for the floating mid-span section of the models having a width of 2.5 in. A detailed description of the modelcon figurations tested is given by Howell.[1]

B. Drag Force Balance

For the purpose of this study a drag force balance was designed and constructed. A schematic diagram and a photograph of the drag force balance taken prior to its installation in the wind tunnel are shown in Fig. 4. The balance consists of a floating element with strain gages mounted on flexure beams. The drag force balance was extensively tested for preciseness and accuracy yielding a linear calibration curve which passed through zero. The calibrations were repeatable to within $\pm\frac{1}{2}\%$.

The drag force balance was tested aerodynamically for accuracy by using a flat plate model 4 in. long by 2.5 in. wide. Average skin friction coefficients measured with this drag balance[12] compared well with typical calculation methods for skin-friction coefficients; e.g., Spalding-Chi,[13] Coles,[14] and Culick-Hill-Howell.[12] These comparisons are shown in Fig. 5.

In contrast to flat plate friction drag measurements, determination of notch drag forces brought into account the pressure differentials arising on the model faces perpendicular to the freestream. Also to be considered was the wall friction force contributed by the flat plate approach length, especially for the smaller notch length models. A detailed discussion of design and calibration of the drag balance is given by Howell.[1]

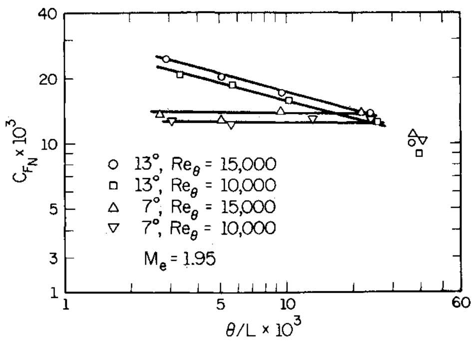

Fig. 7 Effect of boundary-layer thickness on notch drag in supersonic flow.

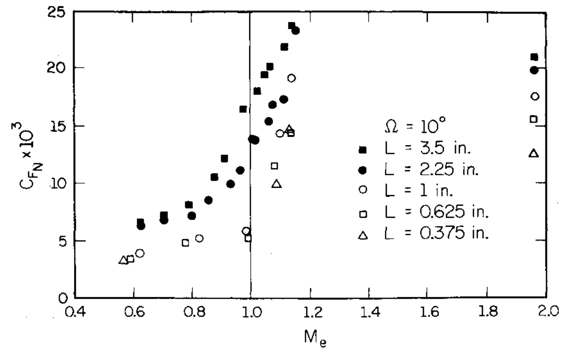

Fig. 8 Transonic drag coefficient for 10° notch of various lengths.

C. Drag Force Measurements

For each of the notches tested two corrections were made in the indicated drag force F_{balance}. The first one to account for the effect of the pressure differential existing in the balance gaps F_{Δ_p} (measured with pressure taps) and the second to account for the friction drag F_{sh} acting on the flat plate portion of the model (by use of the theoretical value). Thus, the true drag force F_N of the notch is given by

$$F_N = F_{\text{balance}} - F_{\Delta_p} - F_{sh}$$

The drag coefficient of the notch is then

$$C_{F_N} = \frac{F_N}{\frac{1}{2}\rho_e U^2 b L} \tag{8}$$

with

$$C_{F_N} = C_{F_N}(M_e, \theta/L, Re_L, \Omega)$$

For each model tested in the supersonic test section, M_e was essentially constant and Re_L (and Re_θ) was the only controlled variable. By selecting different model sizes of length L having the same notch angle Ω, the effect of θ/L and Re_L could be determined. A summary of these results is given in Fig. 6. It is immediately observed that the effect of flow separation not only strongly decreases the drag coefficient below the values representative for wedges corresponding in geometry to the notches, but also that increasing θ/L leads to a sizeable further reduction for notches submerged in boundary layer. These conclusions are borne out by the results given in Fig. 7.

For the transonic tests, the main controlled variable was the Mach number, while the Reynolds number Re_θ variation was coupled to the Mach number variation. The effects of θ/L and Re_L were again observed by using models of different sizes L. Drag coefficients for 10° notches of different lengths L are shown in Fig. 8 as functions of freestream Mach number. Figure 9 depicts the effects of θ/L with Mach number chosen as a parameter.

V. Discussion

The results shown in Figs. 7 and 9 indicate that the Reynolds number effect is of minor importance when compared with other variables. For the supersonic results depicted in Fig. 7, it is clear that the notch angle is a significant factor in the determination of the drag coefficient for $\theta/L < 0.02$, while, for $\theta/L > 0.02$, it is independent of the notch angle. A similar trend for transonic flow can be observed in Fig. 9; however, the discriminating value of θ/L is a function of Mach number.

For purposes of discussion, a thin boundary layer is one in which θ/L is small enough so that the notch angle affects the drag coefficient, while a thick approaching boundary layer is one where the notch drag coefficient is independent of the notch angle. For $1.1 < M_e < 2$,

$$(\theta/L)_{\text{thin}} < 0.02 < (\theta/L)_{\text{thick}}$$

while, for $M_e = 0.6$,

$$(\theta/L)_{\text{thin}} < 0.09 < (\theta/L)_{\text{thick}}$$

A. Thin Approaching Boundary Layers—$M_e \simeq 2$

All of the V-shaped notches tested in the supersonic regime with thin approaching boundary layers exhibited an increase in the drag coefficient with increasing Reynolds number at a constant value of θ/L and Ω (Fig. 7).

The change in C_{F_N} caused by a change in Ω can easily be observed in Fig. 6. For this range of notch length, the notch drag coefficient C_{F_N} increased with increasing notch angle for a given notch length. For comparison purposes, C_D estimates are shown using inviscid linearized supersonic theory for half-diamond-shaped profiles. The progressive deviation of the drag coefficient from the linearized theory solution as Ω was increased demonstrated how the changing flow geometry reduced C_{F_N} from the theoretical solution based on the wall geometry.

A comparison of the experimental results with the solution obtained by using Eq. (6) is displayed in Fig. 10. It is interesting to note from these results that for a given L, the increase of C_D for an increase in Ω above 13° is negligible because the flow separates close to the leading edge of the notch, making the wave drag contribution small in comparison to the shear drag in the developing shear layer region. For very thin

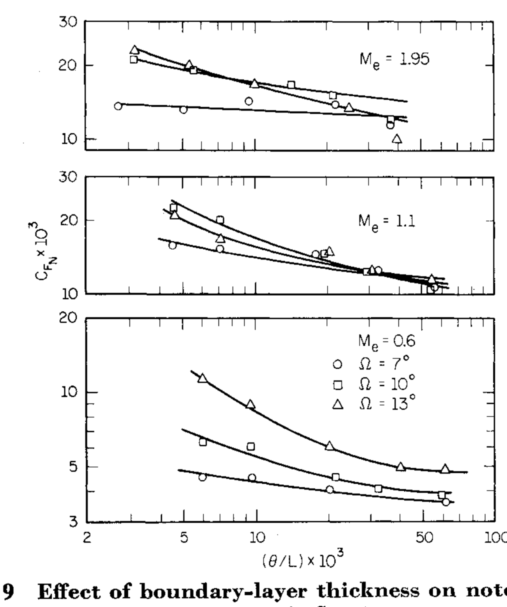

Fig. 9 Effect of boundary-layer thickness on notch drag in transonic flow.

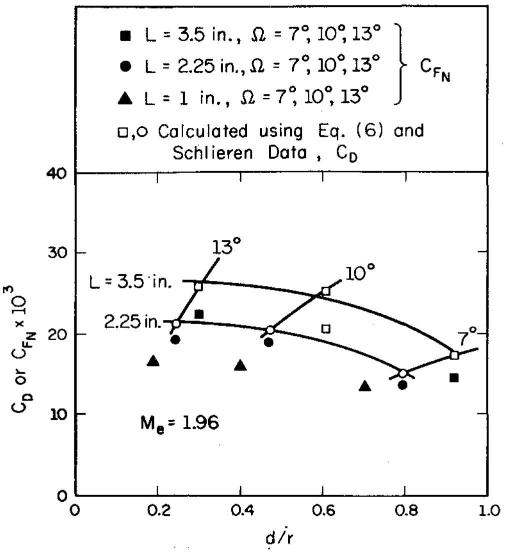

Fig. 10 Comparison of semiempirical model with measured notch drag.

boundary layers ($\theta/L \simeq 0.003$ or $L = 3.5$ in.), the theoretical solution could be extrapolated to a maximum penetration depth ratio ($d/r = 1$) indicating incipient separation for a 6° notch angle.

For thin boundary layers, there is an effect on the drag coefficient as the geometry of the notch is changed. Results in Fig. 7 indicate that, for each value of Ω as θ was reduced, C_{FN} approached a constant value.

In Fig. 11, the ratio of the drag force on different notches to the drag force on a flat plate surface of the same length as the notch D/F is shown for (2.25 in., except for "circular notch") supersonic flow conditions. The 7° notch increased in drag by a factor of five while the 10° and 13° notches have a tenfold increase in drag force. It is interesting to observe the gradual transition from flat plate skin friction to drag of a rectangular notch. It is evident that, if the V-notch angle is greater than 10°, it has practically the same drag force as a rectangular notch which is approximately ten times that of a flat plate. The drag force of a circular cavity with a 0.51 in. mixing length is also shown for comparison.

B. Thin Approaching Boundary Layers—$M_e \simeq 0.6$–1.18

An increase in notch angle resulted in an increase in the drag coefficient for the range of M_e investigated. This effect

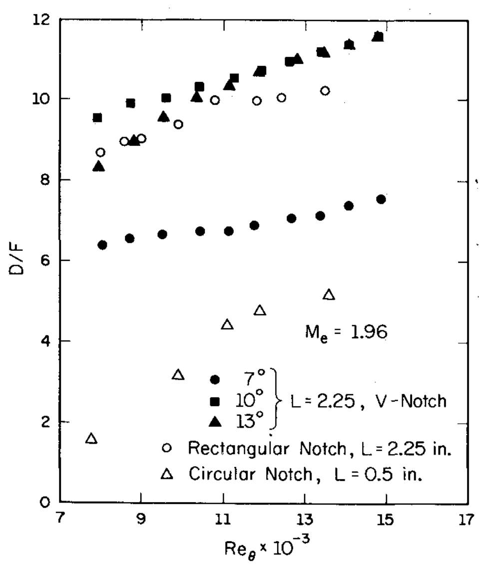

Fig. 11 Ratio of notch—flat plate drag forces.

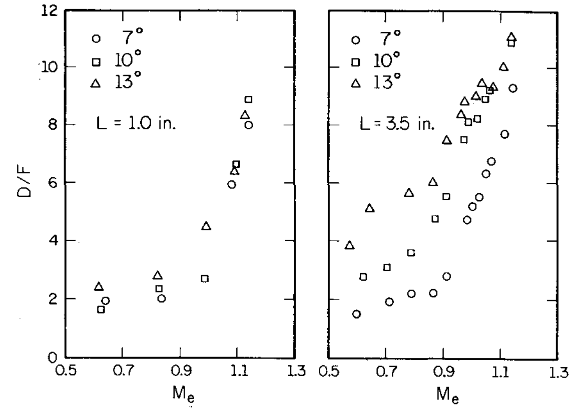

Fig. 12 Ratio of notch—flat plate drag forces for drag forces for transonic flow.

was indicated by the results in Fig. 8 for $L = 3.5$, 2.25, and 1.0 in. notches, which are long enough to be classified as (θ/L) thin. For the transonic flow regime, the same qualitative effect for θ on C_{FN} was observed; however, the results also indicate that the value of θ for which C_{FN} becomes independent of Ω increases for subsonic Mach numbers.

The Mach number effect observed in this investigation was the most pronounced effect, and a portion of the results are illustrated in Fig. 8. It is obvious from these results that a maximum C_{FN} occurs for $M_e > 1$ and that the value of M_e for maximum C_{FN} is dependent on Ω. In Fig. 12, the transition from flat plate skin friction to transonic maximum drag is clearly demonstrated as both the notch angle and size of separated region (notch length) are increased. Again, almost a tenfold increase in drag force is observed.

C. Thick Approaching Boundary Layers—$M_e \simeq 2$

For this classification, there was still an increase in C_{FN} for an increase in Re_θ; however, the change was not as great as $(\theta/L)_{\text{thin}}$. As stated previously, C_{FN} was independent of Ω for $(\theta/L)_{\text{thick}}$. For thick shear layers, the boundary layer acted as a buffer region between the freestream and the solid boundaries with the net effect of reducing the drag coefficient. This reduction is quite obvious in Fig. 7 where as θ/L was increased, C_{FN} was reduced.

D. Thick Approaching Boundary Layers—$M_e \simeq 0.6$–1.18

The drag coefficient is independent of Ω for $(\theta/L)_{\text{thick}}$, while for the range of $M_e > 1.1$ the shear layer effects on C_{FN} were identical to those for $(\theta/L)_{\text{thin}}$. The Mach number effect for transonic thick approaching boundary layers was qualitatively the same as for the transonic thin approaching boundary layers.

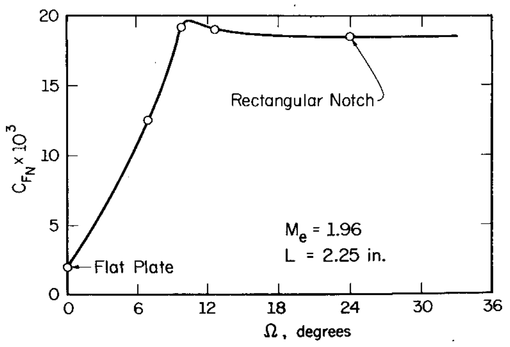

Fig. 13 Flat plate—rectangular notch transition drag coefficient.

VI. Conclusions

From the analytical and experimental results of this investigation, the following conclusions may be made about the drag coefficients for V-shaped notches. 1) The drag force arising from two-dimensional notches has been determined by direct force measurements using a newly developed balance employing strain gages. As depicted in Fig. 13, the effect of notch angle at given M_e and Re_θ is shown to produce a continuous variation from flat plate friction drag values through combined wave drag and free jet mixing contribution to the shear drag in fully separated (square notch) flow regions. 2) A strong effect due to flow separation from the walls of V-shaped notches on the overall flow configuration and drag forces was observed. 3) The effect of the approaching boundary layer can be discussed in two categories, namely, thin or thick, depending on the degree to which the notch angle influences the value of C_{FN}. 4) Reynolds number effects were generally small. 5) Supersonic flow past V-notches with thin approaching boundary layers can be analyzed on the basis of a simplified flow model accounting for the reduction in form drag by introducing information on the penetration depth ratio. 6) Drag values obtained for transonic flow show an anomalous behavior near $M_e = 1$ inasmuch as they reach maximum values at slightly supersonic Mach numbers. 7) The separation point inside the V-notch adjusts itself near $M_e = 1$ resulting in an effective geometry change which reduces the expected notch drag coefficient. 8) Theoretical analysis of the drag of shallow V-notches in the transonic flow regime using empirical information on d/r resulted in good quantitative agreement with measured values.

References

[1] Howell, R. H., "Drag Forces of Two-Dimensional V-Shape Notches in Transonic and Supersonic Turbulent Flow," Ph.D. thesis, 1967, Dept. of Mechanical Engineering, Univ. of Illinois, Urbana-Champaign.

[2] Chang, P. K., *Separation of Flow*, Pergamon Press, London, England, 1970, Chaps. 6 and 7.

[3] Fletcher, L. S., Briggs, D. G, and Page, R. H., "A Review of Heat Transfer in Separated and Reattached Flows," AIAA Paper 70-767, Los Angeles, Calif., 1970.

[4] Charwat, A. F., Roos, J. M., Dewey, F. C., and Hitz, J. A., "An Investigation of Separated Flows—Part I: The Pressure Field, and Part II: Flow in the Cavity and Heat Transfer," *Journal of the Aerospace Sciences*, June 1961, Vol. 28, No. 6, p. 457; Vol. 28, No. 7, July 1961, p. 513.

[5] Kuehn, D. M., "Experimental Investigation of the Pressure Rise Required for the Incipient Separation of Turbulent Boundary Layers in Two-Dimensional Supersonic Flow," Memo 1-21-59A, Feb. 1959, NASA.

[6] Crocco, L. and Lees, L., "A Mixing Theory for the Interaction between Dissipative Flows and Isentropic Streams," *Journal of the Aeronautical Sciences*, Vol. 19, 1952, p. 649.

[7] Lees, L. and Reeves, B. L., "Supersonic Separated and Reattaching Laminar Flows: I. General Theory and Application to Adiabatic Boundary Layer-Shock Wave Interactions," *AIAA Journal*, Vol. 2, No. 11, Nov. 1964, pp. 1907–1928.

[8] Chapman, D. R., Kuehn, D. M., and Larson, H. K., "Investigation of Separated Flows in Supersonic and Subsonic Streams with Emphasis on the Effect of Transition," TN-3896, 1957, NACA.

[9] Korst, H. H., Chow, W. L., and Zumwalt, G. W., "Research on Transonic and Supersonic Flow of Real Fluids at Abrupt Increases in Cross Section," ME TN 392-5, 2nd ed., Oct. 1964, Univ. of Illinois.

[10] Shapiro, A. H., *The Dynamics and Thermodynamics of Compressible Fluid Flow*, Vols. I and II, 1954, Ronald Press, New York, Chap. 14.

[11] Lamb, J. P., "The Development of Free Turbulent Shear Layers," AEDC-TR-65-184, 1965, Arnold Engineering Development Center.

[12] Howell, R. H., "Drag Force Measurements of a Compressible Turbulent Boundary Layer on an Adiabatic Smooth Flat Plate," Paper 70-WA/FE-26, 1970, ASME.

[13] Spalding, D. B. and Chi, S. W., "The Drag of a Compressible Turbulent Boundary Layer on a Smooth Flat Plate with and without Heat Transfer," *Journal of Fluid Mechanics*, Vol. 18, 1964, pp. 117–143.

[14] Coles, D., "The Turbulent Boundary Layer in a Compressible Fluid," *The Physics of Fluids*, Vol. 7, No. 9, 1964, pp. 1403–1423.